https://doi.org/10.5194/hess-2022-418
Preprint. Discussion started: 6 January 2023

Hydrology and Earth System Sciences
Discussions
Open Access
EGU

Throughfall spatial patterns translate into spatial patterns of soil moisture dynamics – empirical evidence

Christine Fischer[1,2], Johanna Clara Metzger[1,3], Gökben Demir[1], Thomas Wutzler[4], Anke Hildebrandt[1,5*]

[1] Institute of Geosciences, Friedrich-Schiller-University Jena, Burgweg 11, D-07749 Jena, Germany
[2] Office for Green Spaces and Waters, City of Leipzig, Prager Straße 118-136, D-04217 Leipzig, Germany
3 Institute of Soil Science, University of Hamburg, Allende-Platz 2, 20146 Hamburg, Germany
[4] Max-Planck-Institute for Biogeochemistry, Jena, Germany
[5] Department Computational Hydrosystems, Helmholtz Centre for Environmental Research - UFZ, Leipzig, Germany
* corresponding author

Abstract

Throughfall heterogeneity induced by the redistribution of precipitation in vegetation canopies has repeatedly been hypothesized to affect the variation of soil water content and runoff behavior, especially in forests. However, we are not aware of any observational study relating the spatial variation of soil water content directly to net precipitation to confirm modelling hypotheses. Here, we investigate whether throughfall patterns affect the spatial heterogeneity of soil water response in the main rooting zone. We assessed rainfall, throughfall and soil water contents (two depths: 7.5 cm and 27.5 cm) on a 1-ha temperate mixed beech forest plot in Germany 2015 - 2016 during the growing seasons in independent high-resolution stratified random designs. Because throughfall and soil water content cannot be measured at the same location, we used kriging to derive the throughfall values at the locations where soil water content was measured. We first explore the spatial variation and temporal stability of throughfall and soil water patterns, and next evaluate the effects of input (throughfall), soil properties (field capacity and air capacity), and vegetation parameters (canopy cover and distance to the next tree) on soil water content and dynamics.

Throughfall spatial patterns were related to canopy density. Although spatial auto-correlation decreased with increasing event sizes, temporally stable throughfall patterns emerged, leading to reoccurring high and lower input locations across precipitation events. A linear mixed effect model analysis showed, that soil water content patterns were only poorly linked to throughfall spatial patterns, and it was rather shaped by unidentified but time constant factors.

Instead of soil water content itself, the patterns of its increase after rainfall corresponded more closely to throughfall patterns, in that more water was stored in the soil where throughfall was elevated. Furthermore, soil moisture patterns themselves enhanced or decreased water storage in the soil, and probably fast drainage and runoff components. Locations with low topsoil water content tended to store less of the input water, indicating preferential flow. In contrast in subsoil, locations with high water content stored less water. Also, distance to the next tree and air capacity modified how much water was retained in soil storage.

In this comprehensive study we show that throughfall patterns imprint less on soil water contents and more on soil water dynamics shortly after rainfall events, therefore only partly confirming previous modelling with data. Our findings highlight at the same time systematic patterns of times and locations where the capacity to store water is reduced and water probably conducted quickly to greater depth. Our results indicate that not soil moisture patterns but rather percolation may depend on small scale spatial heterogeneity of canopy input patterns.

Keywords: throughfall, mixed beech forest, soil water content increase, temporal variation, spatial variation, pattern

https://doi.org/10.5194/hess-2022-418
Preprint. Discussion started: 6 January 2023

Hydrology and Earth System Sciences
Discussions

1. Introduction

Over the past decades, there has been a raised interest on how water input at the soil surface is affected by vegetation canopies to understand and predict hydrological processes related to vegetation structure and land use change (Western et al., 2004; Savenije, 2004; Murray, 2014; Guswa et al., 2020; Oda et al., 2021). Due to interception losses, the water arriving below the canopy is a smaller amount compared to above (Horton, 1919 and references therein; Carlyle-Moses and Gash, 2011) with implications for the soil water balance (Durocher, 1990; Bouten et al., 1992; Schume et al., 2003; Klos et al., 2014; Metzger et al., 2017) and overall water budget at the catchment scale (Brown et al., 2005; Oda et al., 2021).

Next to interception loss, the contact of precipitation with the vegetation canopy causes spatial redistribution of the incoming water. This leads to characteristic spatial heterogeneity of the dripping (thoughfall) and flowing (stemflow) below canopy precipitation, locally causing enhanced water input to the soil surface. For example, hotspots by dripping points (enhanced water flow from peculiarities in the canopy, Falkengren-Grerup, 1989; Keim et al., 2005; Staelens et al., 2006; Voss et al., 2016) and stemflow hotspots (Levia and Germer, 2015; Carlyle-Moses et al., 2018) are well-documented. The available research suggests that both throughfall patterns and stemflow spatial distributions are reoccurring (Keim et al., 2005; Staelens et al., 2006; Zimmermann et al., 2008; Wullaert et al., 2009; Guswa and Spence, 2012; Metzger et al., 2017; Van Stan et al., 2020).

The observed persistence of spatial patterns of below canopy precipitation has created a strong expectation that those affect patterns of soil water content (Schume et al., 2003; Wullaert et al., 2009; Rosenbaum et al., 2012; Zehe et al., 2010) and hotspots of percolation or preferential flow (Bouten et al., 1992; Schume et al., 2003; Blume et al., 2009; Bachmair et al., 2012) in forests soils. Yet, this is only partly confirmed with observations: For stemflow affected locations, soil moisture microsites have repeatedly been demonstrated (Pressland, 1976; Durocher, 1990; Liang et al., 2007; Germer, 2013; Metzger et al., 2021). Stemflow can create substantial funneling of water to the forest floor and water availability on the forest floor can be locally enhanced 10 to 100 times (Levia and Germer, 2015; Carlyle-Moses et al., 2018; Metzger et al., 2021).

While for stemflow the belowground consequences of input hotspots have been repeatedly confirmed, much less research is available about the role of the less pronounced, but still spatially persistent pattern of throughfall for soil water dynamics. Modelling suggested that throughfall patterns influence the root zone soil moisture pattern (Coenders-Gerrits et al., 2013; Guswa, 2012). However, soil moisture patterns are also influenced by several other factors creating substantial heterogeneity such as heterogeneity of soil properties, local micro-topography, litter thickness or root water uptake (Bouten et al., 1992; Schume et al., 2003; Schwärzel et al., 2009; Gerrits and Savenije, 2011; Rosenbaum et al., 2012; Liang et al., 2017; Molina et al., 2019), and those are typically not fully captured in virtual experiments. In contrast, observation studies found that throughfall and root zone soil moisture were not (Shachnovich et al., 2008; Rodrigues et al., 2022) or only occasionally (Metzger et al., 2017) or weakly (Molina et al., 2019) related. On the other hand, Klos et al. (2014) found a relation below the rooting zone by strategically sampling at high and low throughfall positions, and several authors found indirect evidence by interpreting the change of spatial variation in soil water content (Zehe et al., 2010; Rosenbaum et al., 2012; Metzger et al., 2017) after precipitation events.

https://doi.org/10.5194/hess-2022-418
Preprint. Discussion started: 6 January 2023

In light of the substantial heterogeneity of other influencing factors, one of the reasons for the limited direct observational evidence of the effect of throughfall on soil water content maybe the lack of studies investigating the relation between below canopy precipitation and soil water patterns in a dedicated and coordinated fashion. The characterization of spatial patterns, such as those of throughfall, requires a large number of samplers (Kimmins, 1973; Lloyd and Marques, 1988; Zimmermann et al., 2010; Van Stan et al., 2020), and the same is true for below ground observations. Furthermore, a fundamental challenge is that soil water input and soil water content cannot be assessed at the same location, since the throughfall measurements disturb the infiltration into the soil. The objective of this study is therefore to compare the patterns of soil water content, soil properties and throughfall using a dedicated spatially highly resolved sampling design to reveal whether input, next tree distance or soil properties affect spatial variation in soil water content and soil water response. We used independent designs for above and below ground observations and applied kriging to derive the throughfall values at the locations where soil water content was measured. The aims of the study were to a) to explore spatial heterogeneity and temporal stability of throughfall and soil water content and b) evaluate the influence of soil properties (field capacity and macroporosity), vegetation parameters (canopy cover, next tree distance) and input variation (throughfall) on the variation of soil water content and soil water content increase after precipitation.

2. Methods

2.1 Study area

The study was carried out in the Hainich Critical Zone Exploratory (CZE Hainich, see Küsel et al. 2016), run by the Collaborative Research Centre "AquaDiva". The site is located in Central Germany, in the Hainich National Park in an unmanaged beech dominated forest. Mean annual temperature are around 7.5 to 9.5 °C, depending on the position of the small mountain, and the and total annual precipitation drops from 900 to less than 600 mm from ridge to valley (Küsel et al., 2016). The monitoring site as well as measurements of precipitation and soil moisture has been described in Metzger et al. (2017), the important parts are repeated here for completeness. The site covers an area of 1 ha and is situated at 365 m a.s.l.. The study area contains of 581 tree individuals (diameter breast height ≥ 5 cm), representing a heterogeneous age structure. The soils in this area are dominatly luvisols (Schrumpf et al., 2014; Kohlhepp et al., 2017). The species assemblages consists of 70% European beech trees (*Fagus sylvatica*), as well as Sycamore maple (*Acer pseudoplatanus*), European ash (*Fraxinus excelsior*), European hornbeam (*Carpinus betulus*), Large-leafed linden (*Tilia platyphyllos*), Norway maple (*Acer platanoides*) and Scots elm (*Ulmus glabra*). The weathered bedrock is at 15 to 87 cm depth (median depth 37 cm). More details on the research site are given in Metzger et al. (2017).

2.2 Precipitation measurements and processing

The precipitation sampling follows the same procedure as given in Metzger et al. (2017). Gross precipitation (P_g) and throughfall (P_{TF}) were measured manually using gauges on a per-event basis in spring 2014, 2015, 2016. The current analysis covers the period from June 18 to July 28 2015 and May 31 to July 14 2016. The installed throughfall collectors consist of circular funnels (diameter = 12 cm), the opening of which is placed about 37 cm above the ground surface. A table tennis ball is placed in the opening of the funnel to minimized evaporation.

https://doi.org/10.5194/hess-2022-418
Preprint. Discussion started: 6 January 2023

Hydrology and Earth System Sciences
Discussions
Open Access
EGU

125 Throughfall collectors were arranged in a stratified sampling design (Zimmermann et al., 2016). For this, the 1 ha
126 plot was divided into 100 subplots each 10 m x 10 m (Figure 1) and equipped with two randomly located
127 throughfall samplers. Of those, we selected 50 point randomly and added another sampler in direct vicinity (0.1 m
128 distance) creating a "short transect". Furthermore, to 25 randomly selected short transects we added four more
129 samplers at 0.5, 1, 2, and 3 m from the first to form "long transects". The direction of all transects was also
130 randomly chosen. In total we sampled n = 350 throughfall positions.
131 Sampling started 2 h after the end of rainfall by collecting the volume of all sampling containers using graduated
132 cylinders. Gross precipitation was measured at an adjacent (distance 250 m) open grassland using five funnels of
133 the same type as the throughfall collectors.

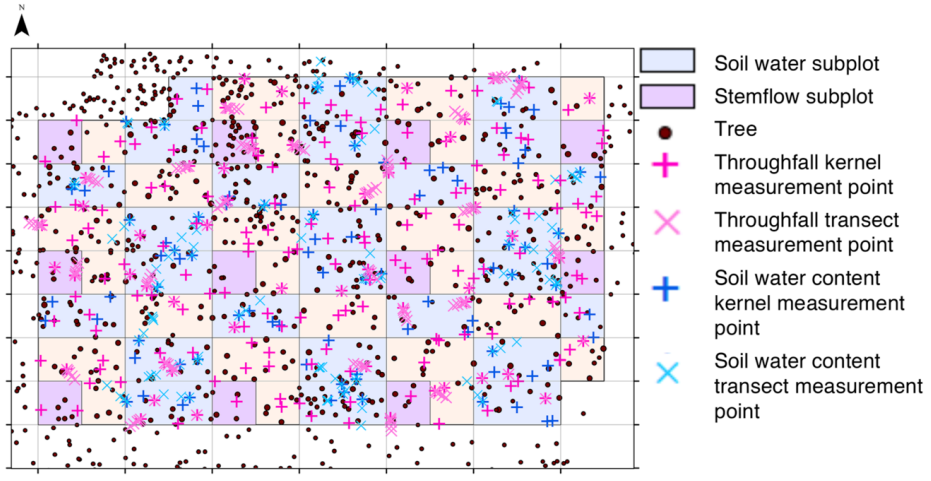

134
135 Fig. 1: Experimental set-up in the 1-ha forest plot subdivided by a 10 m x 10 m grid yielding 100 subplots.
136 Positions of the throughfall samplers (pink crosses) and 49 soil water content subplots (blue) measured in a
137 stratified random design with transects (see material and methods for more details, Figure from Metzger et al.,
138 2017).
139
140 To allow comparison of spatial pattern between events, we calculated a normalized spatial deviation of each
141 measurement ($\delta P_{\mathrm{TF,i}}$) similarly to Vachaud et al. (1985). Since throughfall is not always normally distributed in
142 space, we used the median ($\hat{P}_{TF}$) instead of the arithmetic mean for normalization, as already done by Zimmermann
143 et al. (2008) and Wullert et al. (2009) as follows
144

$$\delta P_{\mathrm{TF,i}} = \frac{P_{\mathrm{TF,i}} - \hat{P}_{TF}}{\hat{P}_{TF}} \quad (1)$$

145 where $\delta P_{\mathrm{TF,i}}$ represents the normalized value of the spatially distributed measurements of throughfall ($P_{\mathrm{TF,i}}$) at
146 locations i for a specific event, and $\hat{P}_{TF}$ the spatial median for that event. To investigate the temporal persistence
147 of the spatial pattern of throughfall we derived temporal stability plots (Zimmermann et al., 2008; Wullaert et al.,
148 2009) by ranking the normalized throughfall from minimum to maximum. Additionally, we calculated Spearman
149 rank correlation coefficients between observations of different events, where high correlations indicate strong

https://doi.org/10.5194/hess-2022-418
Preprint. Discussion started: 6 January 2023

Hydrology and Earth System Sciences
Discussions

persistence (or temporal stability) of the throughfall pattern. We paired all events falling into a given rain event class according the Metzger et al. (2017): small: ($P_g \leq 3$ mm); medium (3 mm $< P_g \leq 10$ mm), large ($P_g > 10$ mm). To relate the general precipitation and soil moisture conditions during the observation period to the average climate, we compared them with precipitation data from a nearby gauge (Mühlhausen- Windeberg, 20 km to the northeast) of the German Weather Service (DWD climate data centre, www.dwd.de/cdc, ID 5593).

2.3 Soil water content measurements

The soil water measurements were first described in Metzger et al. (2017). Volumetric soil water content was monitored using a wireless sensor network (SoilNet, Bogena et al. (2010)) equipped with SMT100 frequency domain sensors (Truebner GmbH, Neustadt, Germany). Overall 210 soil water content measurement points were distributed in a stratified random design in the blue subplots shown in Figure 1: Within each blue subplot, two sampling points were placed randomly. Additionally, to a subset of 24 randomly selected points, transects were added with three additional measurement points (at 0.1, 2.0, and 6.0 m from the position). Furthermore, 40 locations were added as transects near tree stems. At each soil moisture measurement location, sensors were installed in two depth, e.g topsoil 7.5 cm and subsoil 27.5 cm depth. For this analysis we used the data collected during the throughfall measurement campaigns from June 18 to July 28 2015 and May 31 to July 14 2016. At each locations, we used soil moisture measurements an hour preceding the observed rain event ($\theta_{pre,i}$) to characterize soil moisture and its pattern in the drained state and the maximum soil water content induced by the rain event ($\theta_{post,i}$) to characterize the post event state. We also assessed the soil water content response by calculating the change of soil water content ($\Delta\theta_i$) for each event and each location with

$$\Delta\theta_i = \theta_{post,i} - \theta_{pre,i} \quad (2)$$

where positive values of $\Delta\theta_i$ indicate water content increase.

Equivalently to throughfall, we calculated the median soil water contents ($\hat{\theta}_{\mathrm{pre}}$, $\hat{\theta}_{\mathrm{post}}$) as well the relative deviations ($\delta\theta_{pre,i}$, $\delta\theta_{post,i}$), indicating the spatial pattern of soil water content according to Equation 1. Using the normalized values of soil water content and throughfall next to the medians in the statistical models (see below) allowed us to differentiate between spatial patterns and temporal variation across events.

2.4 Canopy and soil property measurements

At the time of soil sensor installation, undisturbed soil samples were collected using metal ring cylinders with a volume of 100 cm^3. The distance between the sensor position and the soil sample collection was approximately 0.5 m. Soil properties were treated as if they were measured directly at the soil sensor location i. In order to determine field capacity ($\theta_{FC,i}$), the samples were first saturated and next let drain in a sand box with a hanging water column imposing a pressure of −60 hPa for 72 hours and weighed. The soil cores were subsequently dried for 24 h at 105° C and weighed again to obtain the dry weight $m_{dry,i}$. The volumetric water content at field capacity ($\theta_{FC,i}$) was derived from the weight difference of the sample at -60 hPa and the dried one, while assuming a density of water of D_w = 1 g cm^{-3}. Bulk density ($D_{bd,i}$) was calculated from soil dry weight and volume. Soil apparent porosity (φ_i) was calculated from the bulk density and assuming a constant density of the soil mineral component (D_m = 2.66 g cm^{-3})

https://doi.org/10.5194/hess-2022-418
Preprint. Discussion started: 6 January 2023


Hydrology and Earth System Sciences
Discussions
Open Access
EGU

$$\varphi_i = 1 - \frac{D_{bd,i}}{D_m} \quad (3)$$

Air capacity ($\theta_{AC,i}$, also called air-filled porosity) was then determined as

$$\theta_{AC,i} = 1 - \theta_{FC,i} \quad (4)$$

To characterize the canopy density, we counted the number of branches (canopy cover) above the throughfall samplers in 2014. This data was however not available for soil water measurement locations.

2.5 Statistical Analysis

All statistical analysis were processed with R 3.2.3 (Core Team 2016). For the geostatistical analysis (detailed below) we used the the packages *geoR* (Ribeiro Jr and Diggle, 2001), *georob* (Papritz and Schwierz, 2020) and *gstat* (Pebesma, 2004; Gräler et al., 2016). Linear mixed effects models were implemented using the package *lme4* (Bates et al., 2015) and *lmerTest* (Kuznetsova et al., 2017). The variance explained by fixed and random factors (conditional R^2) and by only fixed effects (marginal R^2, Nakagawa and Schielzeth (2013)) for the final model were calculated with the *MuMIn* package (Barton, 2020).

2.5.1 Geostatistical estimation of throughfall

Throughfall was estimated at the soil water content measurement locations by kriging. The overall procedure for obtaining the variograms closely follows Zimmermann et al. (2016) with some adaptations taken from Voss et al. (2016). Important steps and decisions of the exploratory data and geostatistical analysis are shown in Figure S1.

1. Exploratory Analysis-Test for trends and underlying asymmetry. First, we determined the skewness using the octile skew. The octile skew of none of the throughfall events was larger than 0.2 or smaller -0.2 and we therefore did not transform the data. If a spatial trend existed ($p \leq 0.150$), we used the residuals of the spatial regression model for the coordinates x and/or y instead of the real data in the following.

2. Variogram estimation by the method-of-moments (MoM). We calculated the empirical throughfall variogram using both non-robust and robust estimators (Matheron, 1962; Cressie and Hawkins, 1980; Dowd, 1984; Genton, 1998) using the *sample.variogram* function in the package *georob* in R. For throughfall we chose lags centered at 0.125, 0.375 and 0.75, followed by a step size of 1 m up to 50 m). Next, we obtained a provisional variogram, which serves for spatial outlier detection in step 3. For this, we fitted three models to the experimental variogram (spherical, exponential and pure nugget) using *fit.variogram.model* function in the package *gstat* and chose the model with the lowest Residual Sum of Squares. Then we assessed the fitted model by leave-one-out cross validation. Based on this we calculated the normalized kriging error (Θ_i,) (Lark, 2000) and compared the variograms from all mentioned estimators using the estimator with a median of Θ nearest to 0.455 (Zimmermann et al., 2008).

3. Identification and spatial outlier removal. Before final variogram estimation using residual maximum likelihood (REML) in step 4, outliers were removed based on kringing and cross validation using the provisional variagram obtained in step 2. For identifying a spatial outlier at location *i* we used the standardized error of cross validation $\varepsilon_{s,i}$ (Bárdossy and Kundzewicz, 1990, Lark, 2002). To classify an outlier we used the *Z*-statistics. Sampled points with $\varepsilon_{s,i} < -2.576$ ($\alpha/2 = 0.005$) were removed (Zimmermann et al., 2016).

https://doi.org/10.5194/hess-2022-418
Preprint. Discussion started: 6 January 2023

4. Variogram estimation by residual maximum likelihood (REML). After outlier removal, we applied REML to fit the theoretical model including spatial trend if necessary, using the *likfit* function in the package *geoR*. We used the initial estimates from the provisional variogram (step 2) for the parameters sill, nugget and range. The range relates to the distance over which the observations are still spatially correlated. In the following, we will use the term correlation length to refer to the effective range, e.g. the distance at which the variogram approaches the sill to 95%. For example, a high effective range indicates a high spatial correlation between the throughfall collectors. We checked the reliability of the final model with the statistic Θ_i (see above).

5. Kriging. Using the final variogram from step 4, we applied ordinary kriging to predict throughfall values at the soil water content measurement locations. Locations where the kriging variance exceeded 95% of the spatial variance were removed from further analysis.

2.5.2 The coefficient of quartile variation (CQV)

We used quantile based statistical metrics for descriptive statistics and correlation since throughfall and soil moisture patterns are commonly skewed (Famiglietti et al., 1998; Zimmermann and Zimmermann, 2014), and throughfall typically includes extreme values due to dripping points (Falkengren-Grerup, 1989; Keim et al., 2005; Staelens et al., 2006; Voss et al., 2016). For the coefficient of variation, we used the quartile variation coefficient (CQV) (Bonett, 2006) as alternative to the coefficient of variation:

$$CQV = \frac{Q3 - Q1}{Q3 + Q1}$$

where Q1 and Q3 represent first and third quartiles. Like the classical coefficient of variation, the CQV is dimensionless statistical measure that describes the relative degree of scattering of the sample.

2.5.3 Linear mixed effects models calculation

We applied linear mixed effect models (LME) with repeat-measurement structure to evaluate the influence of potential drivers explaining soil water content or soil water content increase. We present results on the following dependent variables: Spatial pattern of pre-event ($\delta\theta_{pre}$), and post-event ($\delta\theta_{post}$) soil water content as well as soil water content increase ($\Delta\theta$).

The independent variables (fixed effects) for $\delta\theta_{pre}$ were: Gross precipitation (P_g), nearest tree distance (d_{tree}), air capacity (θ_{AC}), field capacity (θ_{FC}), throughfall of the preceding event (P_{TFpre}). The independent variables (fixed effects) for $\Delta\theta$ and $\delta\theta_{post}$ were: Gross precipitation (P_g), spatial median of soil pre-event water content ($\hat{\theta}_{pre}$), spatial pattern of soil pre-event water content ($\delta\theta_{pre}$), nearest tree distance (d_{tree}), air capacity (θ_{AC}), field capacity (θ_{FC}), spatial median of throughfall ($\hat{P}_{TF}$) and spatial pattern of throughfall (δP_{TF}). Year, day of year and sensor position were implemented as random effects accounting for repeated measurements. To avoid model over-fitting it is important that there are no strong correlations between the explanatory variables (Graham, 2003). To detect multi-collinearity and to avoid potentially spurious models we calculated Spearman rank correlation coefficients (ρ) for all pairs of predictors (Table S1). Before the analysis we removed one of a pair of highly correlated predictors: Gross precipitation (P_g, strong correlation with $\hat{P}_{TF}$) and field capacity (θ_{FC}, strong correlation with θ_{AC}). All predictor variables were normalized. To obtain the minimal adequate models for the response variables,

https://doi.org/10.5194/hess-2022-418
Preprint. Discussion started: 6 January 2023


Hydrology and Earth System Sciences
Discussions

we started with the maximum model and removed stepwise all non-significant terms based on the Akaike Information Criterion (AIC). Main effects included in significant interactions were retained in the model.

3. Results

3.1 Precipitation, throughfall and soil water content pattern

The summer rainfall (May to October) for the last 30 years (1986 – 2016) shows an average of 352 mm (Mühlhausen-Windeberg). During the two summer periods of this study (2015 and 2016), the annual rainfall was below the long-term mean (276 and 303 mm, respectively). However, the summer 2015 were the third driest of the last 30 years (Metzger et al., 2017). The final winter months of 2014 were the driest and the hydrological year 2014/2015 the second driest of the 30 years period. The hydrological year 2015/2016 and the final winter months of 2015 received average precipitation.

Descriptive statistics of throughfall and soil water content (topsoil and subsoil) are given in Table 1. We observed 14 rainfall events in 2015 and ten in 2016. The gross precipitation ranged between 1.6 and 35.2 mm, with three small, six medium and five large in 2015, and one medium and nine large events in 2016. For both years, soil water content increased with soil depth (Table 1). The soil water content increase (difference between post-event and pre-event soil water content; $\Delta\theta$) was always higher in the topsoil compared to the subsoil. For smaller rainfall events, an increase in soil water content was mainly limited to the topsoil, and only following larger rainfall event, in both soil depths.

3.2 Spatial pattern of throughfall

The model parameters fitted to the semi-variograms in the separate steps indicated in Section 2.5.1 are shown in Table S2-4 and correlation lengths (effective range) of the final variograms (step 4, Table S4) are shown in Figure 2. Throughfall correlation lengths decreased with increasing event size from on average 6.2 m for large events to 7.5 m for medium and 9.5 m for small events. In comparison, canopy density correlation length was 7.5 m, i.e. similar to medium events. Throughfall and canopy density had a small nugget and a strong spatial dependence (nugget/sill ratio < 25%) for all events (Table S4). For both years, throughfall decreased significantly with increasing canopy density (Table S5), although most of the variance for spatial patterns of throughfall was related to unknown random effects.

The spatial variation of throughfall (inter-quartile range) increased with event throughfall, but the coefficient of quartile variation (CQV), which normalizes by event size, decreased (Table 1). The high Spearman rank correlation coefficient indicates a strong similarity of the spatial distribution of throughfall between individual events of the same size class (Figure 3). Thus, throughfall produced persistent wet and dry spots, also confirmed by time stability plots (Figure S2).

Soil water content spatial variation coefficients (CQV) decreased with increasing soil water content (expressed as the spatial mean) and consequently with increasing soil depth (Table 1, Figure S3). In the topsoil, the relation was more concave for post-event soil water content (Figure S3) compared to pre-event soil water content, indicating that the event response enhanced soil water content variation especially in drier (summer) conditions in topsoil. However, the by far highest CQV were observed for the increase in soil water content after rain ($\Delta\theta$).

https://doi.org/10.5194/hess-2022-418
Preprint. Discussion started: 6 January 2023

Table 1: Overview of observed rainfall event properties. Event date, gross precipitation (P_g), spatial statistics of throughfall (P_{TF}), soil water content before (θ_{pre}) and after (θ_{post}) the rain event, as well as the soil water content increase ($\Delta\theta$) in topsoil and subsoil: spatial median (med), coefficient of quartile variation (CQV), interquartile range (IQR), and effective range (Range).

Date	***Precipitation***						***Topsoil water content***						***Subsoil water content***					
	P_G	***Event size***	P_{TF}				θ_{pre}		θ_{post}		$\Delta\theta$		θ_{pre}		θ_{post}		$\Delta\theta$	
			med	CQV	IQR	Range	*med*	CQV	med	CQV	med	CQV	med	CQV	med	CQV	med	CQV
	mm		mm	-	mm	m	Vol-%	-	Vol-%		Vol-%	-	Vol-%	-	Vol-%	-	Vol-%	-
21.07.2015	1.6	small	0.6	0.29	0.4	9.6	21	0.16	21	0.17	0.08	2.6	36	0.10	36	0.10	-0.04	-3.34
20.06.2015	2.1	small	0.4	0.60	0.5	9.8	19	0.15	19	0.15	0.00	5.0	30	0.13	30	0.13	0.30	0.27
30.05.2015	2.8	small	1.7	0.21	0.7	9.2	27	0.14	27	0.14	0.03	1.0	37	0.11	38	0.11	0.00	-1.00
18.06.2015	3.3	medium	1.8	0.28	1.0	5.8	19	0.15	20	0.16	0.03	1.0	31	0.13	31	0.13	0.00	-1.47
13.07.2015	3.3	medium	1.9	0.22	0.8	8.6	17	0.14	17	0.14	-0.02	41.0	27	0.14	27	0.15	-0.01	-
02.06.2015	3.7	medium	1.8	0.25	0.9	8.0	27	0.15	27	0.15	0.00	3.0	37	0.12	37	0.12	0.00	-
13.05.2015	4.1	medium	2.7	0.19	1.0	7.6	34	0.11	35	0.10	0.71	0.89	41	0.08	41	0.08	-0.01	-1.00
11.07.2015	4.6	medium	2.7	0.13	0.7	8.9	17	0.14	18	0.13	0.13	1.00	27	0.14	28	0.14	0.72	0.32
25.07.2015	5.7	medium	3.9	0.14	11	4.6	19	0.13	21	0.14	0.41	0.98	33	0.11	33	0.11	0.00	-3.00
15.07.2015	10.5	large	6.6	0.18	2.4	5.9	17	0.14	19	0.17	1.5	0.76	27	0.14	28	0.14	0.33	0.65
08.07.2015	13.3	large	9.4	0.08	1.50	4.8	17	0.14	19	0.15	2.0	0.78	28	0.13	29	0.13	0.28	0.87
28.07.2015	20.1	large	13.7	0.16	4.4	7.5	19	0.13	23	0.21	4.1	0.57	32	0.12	35	0.12	2.60	0.71
24.06.2015	23.0	large	14.2	0.15	4.4	7.0	19	0.15	24	0.21	5.2	0.66	30	0.13	31	0.13	0.27	0.86
20.07.2015	35.2	large	29.2	0.06	3.5	5.9	16	0.15	22	0.19	6.4	0.56	27	0.14	33	0.14	5.43	0.65
28.06.2016	5.3	medium	2.6	0.25	1.3	7.8	26	0.13	25	0.14	0.00	-1.00	35	0.11	35	0.11	0.00	-1.00
21.06.2016	13.7	large	10.1	0.13	2.6	8.9	34	0.10	38	0.09	3.90	0.23	39	0.09	42	0.09	1.56	0.53
06.06.2016	16.9	large	14.9	0.09	2.8	3.0	34	0.09	39	0.09	4.33	0.31	41	0.09	43	0.08	1.58	0.43
02.08.2016	19.6	large	13.7	0.11	3.1	5.7	20	0.13	22	0.19	2.17	0.81	30	0.13	31	0.13	0.12	0.99
04.07.2016	19.8	large	11.9	0.14	3.4	9.5	23	0.14	25	0.16	1.60	0.83	32	0.11	33	0.11	0.01	1.51
25.05.2016	20.8	large	13.3	0.11	3.1	6.5	26	0.12	33	0.15	5.77	0.50	37	0.11	39	0.11	0.74	0.96
16.06.2016	23.2	large	15.2	0.11	3.3	7.3	35	0.12	37	0.10	2.21	0.27	40	0.09	10	0.09	0.01	5.84
14.07.2016	24.1	large	20.0	0.10	4.0	5.0	22	0.17	23	0.20	0.99	0.89	39	0.09	42	0.09	2.81	0.50
31.05.2016	25.0	large	21.0	0.11	4.4	4.6	30	0.12	39	0.09	8.05	0.21	39	0.09	43	0.09	3.98	0.38
25.07.2016	33.5	large	25.6	0.13	6.6	3.5	22	0.15	23	0.18	0.42	0.96	33	0.13	35	0.13	1.34	0.48
	2.2	small	0.9	0.4	0.54	9.5	22	0.15	23	0.15	0.04	2.87	34	0.11	35	0.11	0.09	-1.36
	4.3	medium	2.5	0.2	0.95	7.3	23	0.15	23	0.15	0.2	6.67	33	0.11	33	0.11	0.11	-1.23
	20.3	large	14.8	0.1	3.54	5.6	23	0.13	27	0.15	3.27	0.62	34	0.11	36	0.11	1.40	0.82

https://doi.org/10.5194/hess-2022-418
Preprint. Discussion started: 6 January 2023

Hydrology and Earth System Sciences
Discussions

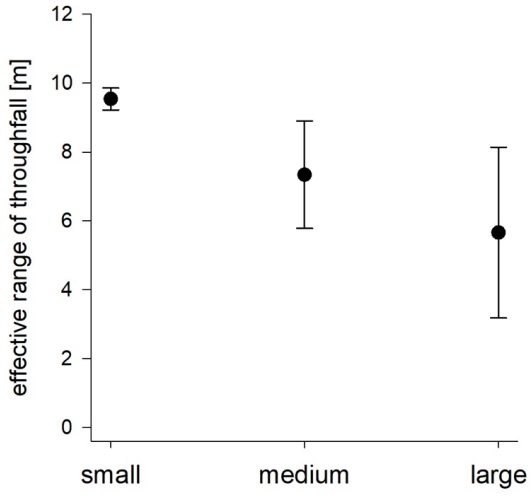

Fig. 2: Comparison of the correlation length, given as effective range, derived from the throughfall variogram calculated for small ($P_g < 3$ mm), medium (3 mm < P_g < 10 mm), large ($P_g > 10$ mm) events.

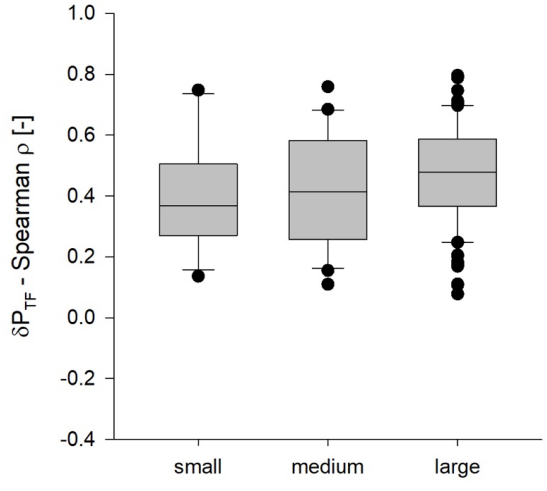

Fig. 3: Temporal stability of the spatial throughfall patterns. Shown are the pairwise correlation coefficients (Spearman) between throughfall (normalized deviation from the plot median (δP_{TF})) from different precipitation events, grouped by event size class (small (n=11), medium (n=21), large (n=91) events.

https://doi.org/10.5194/hess-2022-418
Preprint. Discussion started: 6 January 2023

Hydrology and Earth System Sciences
Discussions
Open Access
EGU

318 The pairwise correlation coefficients indicating the temporal stability of the spatial patterns were high for pre-
319 event (drained) soil water content (θ_{pre}) both in topsoil (Figure 4a) and subsoil (Figure 4b) with $\rho \approx 0.78$. For post-
320 event soil water content (θ_{post}) they were significantly lower in the topsoil ($\rho = 0.70$, Figure 4c) than subsoil
321 ($\rho = 0.77$, Figure 4d) (Mann-Whitney-U Test: $Z = -3.15$, $p = 0.002$). In the topsoil they decreased with increasing
322 event size, revealing patterns were less similar after large precipitation events (Figure 4a,c). In contrast, patterns
323 in soil water content increase after rain events ($\Delta\theta$) were much more weakly correlated with each other (Figure
324 4e,f). However, the similarity of the patterns increased with event size especially in topsoil (Figure 4e), confirming
325 reoccurring wetting patterns especially following larger events.

326

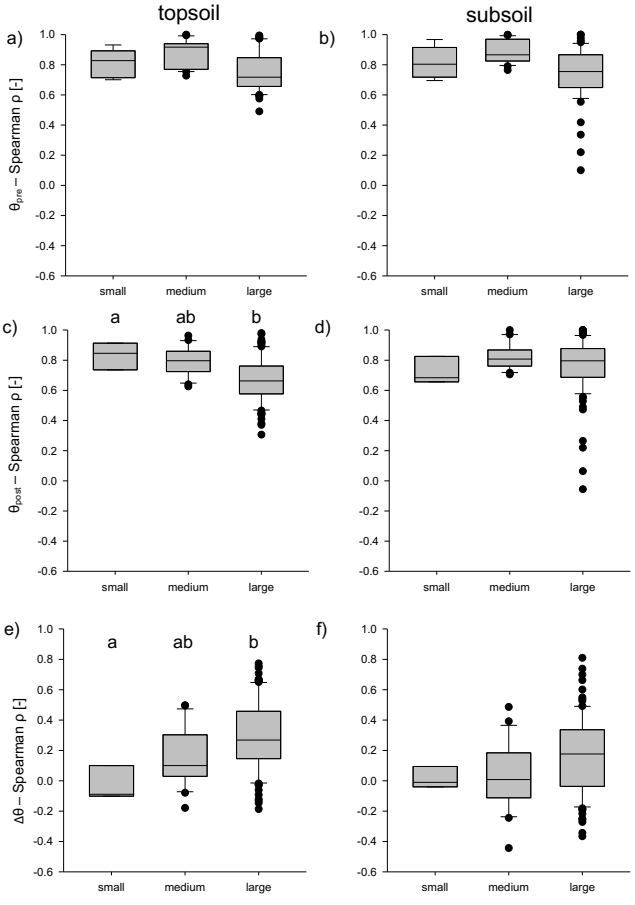

327

328 **Fig. 4**: Temporal autocorrelation of spatial patterns of pre- and post-event soil water content and increase of soil
329 water content after rainfall calculated as pairwise correlation coefficients (Spearman ρ) between all of the
330 different precipitation events within the event size class (small (n = 3), medium (n = 21), large (n = 91). (**top**)
331 pre-event soil water content (θ_{pre}); (**middle**) post-event soil water content (θ_{post}); (**bottom**) increase of soil water
332 content ($\Delta\theta_i$); (**left**) topsoil; (**right**) subsoil. The differences between the events were examined using the Duncan
333 post hoc test of a one-way ANOVA. Letters on the top of bars indicate significant difference ($p \leq 0.05$) between
334 the groups.

https://doi.org/10.5194/hess-2022-418
Preprint. Discussion started: 6 January 2023

Hydrology and Earth System Sciences
Discussions

3.3 Factors influencing soil water spatial distribution

3.3.1 Soil water content

In order to identify the basic drivers for the patterns of soil water content in the drained state ($\delta\theta_{pre}$), we used mixed effects model selection. The resulting best models for top- and subsoil are given in Table 2. The variance explained by fixed effects (marginal R^2) was low, whereas the variance explained by fixed and random effects together (conditional R^2) was high. The model for the subsoil showed an even higher marginal R^2 compared to the topsoil, and a somewhat higher influence of fixed effects. The most important effect identified for topsoil and subsoil was air capacity, with lower soil water content ($\delta\theta_{pre}$) related to locations of higher air capacity (Table 2). In the topsoil also the throughfall of the preceding precipitation event slightly affected the soil moisture pattern. The results for the soil water content itself in the drained state (θ_{pre}) are similar to those of $\delta\theta_{pre}$, except that fixed effects explain even less variation (Table S6).

Table 2: Factors affecting pre-event soil water content patterns ($\delta\theta_{pre}$) in topsoil and subsoil. Results for the best linear mixed effects model. Significant effects are highlighted in bold.

	topsoil		subsoil	
Explained variation				
R^2 Full model	0.818		0.822	
R^2 Fixed	0.035		0.143	
R^2 Random	0.783		0.679	
	t-value	p-value	t-value	p-value
Fixed effects				
Air capacity, θ_{AC}	-2.5	***0.013***	-3.7	***<0.001***
Throughfall of previous event, $P_{TF,\,prev}$	2.3	***0.039***	-1.5	0.161
Tree distance, d_{tree}	-0.8	0.426	1.8	*0.065*
Interactions				
$P_{TF,prev}$ x θ_{AC}	-	-	-2.7	***0.007***
$P_{TF,\,prev}$ x d_{tree}	-2.0	***0.047***	-	-
θ_{AC} x d_{tree}	-	-	1.9	*0.057*

The results of the best linear mixed effects model relating soil water content after a precipitation event to potential drivers is given in Table 3. The spatial pattern of soil water content before the rain event ($\delta\theta_{pre}$) was the major control on either absolute values of spatially distributed soil water content after the rain event (θ_{post}, Table 3) or its spatial pattern ($\delta\theta_{post}$, Table S8). Other fixed ($\hat{P}_{TF}$, δP_{TF}, $\hat{\theta}_{pre}$, θ_{AC}, d_{tree}) and random effects explained only a very small part of the variation.

https://doi.org/10.5194/hess-2022-418
Preprint. Discussion started: 6 January 2023

Table 3: Factors influencing soil water content after a precipitation event (θ_{post}). Results for the best linear mixed effects model including all data (left columns) and grouped by event size (small, medium and large, right columns). Significant effects are shown in bold and effects that were significant in both soil depth (based on all events) are highlighted in grey. Variables are scaled such that the t-value indicates the effect strength. Pseudo R^2 values are given separately for fixed and random effects.

	topsoil								subsoil							
	All events		Small events		Medium events		Large event		All events		Small events		Medium events		Large events	
Full model R^2	0.90		0.99		0.96		0.83		0.89		0.86		0.92		0.92	
Fixed effects R^2	0.87		0.99		0.96		0.76		0.88		0.86		0.92		0.91	
Random effects R^2	0.03		0.00		0.00		0.07		0.00		0.00		0.00		0.01	
	t-value	p-value	t-value	p-value	t-value	p-value	t-value	p-value	t-value	p-value	t-value	p-value	t-value	p-value	t-value	p-value
Fixed effects																
Median event throughfall, $\hat{P}_{TF}$	2.2	***0.035***	4.1	***<0.001***	2.8	***0.007***	1.2	0.238	-0.6	0.494	-	-	-3.0	***0.003***	-1.6	0.141
Spatial throughfall pattern, $\delta P_{TF,i}$	1.8	*0.072*	-	-	2.0	*0.051*	1.9	*0.062*	3.0	***0.003***	-	-	0.8	0.408	3.0	***0.003***
Initial median soil water content, $\hat{\theta}_{pre}$	-1.7	0.106	-4.0	***<0.001***	-2.3	***0.038***	-2.5	***0.024***	-1.4	0.184	-	-	-1.2	0.211	0.6	0.582
Spatial pattern of initial soil water content, $\delta\theta_{pre,i}$	76.4	***<0.001***	200.0	***<0.001***	97.2	***<0.001***	39.2	***<0.001***	98.4	***<0.001***	41.4	***<0.001***	79.2	***<0.001***	59.7	***<0.001***
Tree Distance, d_{tree}	1.8	*0.081*	-	-	-	-	0.9	0.394	-	-	-	-	-	-	0.7	0.498
Air capacity, $\theta_{AC,i}$	-	-	-	-	-2.5	***0.013***	-	-	-2.1	***0.042***	-	-	-	-	-2.2	***0.035***
Interactions																
$\hat{P}_{TF}$ x $\delta P_{TF,i}$	2.3	***0.019***	-	-	-	-	-	-	2.0	***0.048***	-	-	2.0	***0.043***	-	-
$\hat{P}_{TF}$ x $d_{tree,i}$	-1.5	0.129	-	-	-	-	-2.4	***0.015***	-	-	-	-	-	-	-2.2	***0.026***
$\hat{P}_{TF}$ x $\hat{\theta}_{pre}$	-	-	-	-	-	-	-	-	-	-	-	-	-	-	-	-
$\hat{P}_{TF}$ x $\delta\theta_{pre,i}$	-9.7	***<0.001***	-2.5	***0.011***	-	-	-2.2	***0.027***	-2.1	***0.032***	-	-	-5.7	***<0.001***	-2.6	***0.010***
$\hat{P}_{TF}$ x $\theta_{AC,i}$	-	-	-	-	-	-	-	-	-	-	-	-	-	-	-	-
$\theta_{AC,i}$ x $\delta P_{TF,i}$	-	-	-	-	-	-	-	-	-3.4	***<0.001***	-	-	-	-	-3.7	***<0.001***
$\theta_{AC,i}$ x d_{tree}	-	-	-	-	2.3	***0.021***	-	-	-	-	-	-	-	-	-	-
$\theta_{AC,i}$ x $\delta\theta_{pre,i}$	-	-	-	-	-	-	-	-	2.9	***0.003***	-	-	-	-	3.6	***<0.001***
$\hat{\theta}_{pre}$ x $\delta P_{TF,i}$	-2.0	***0.019***	-	-	-	-	-	-	-2.8	***0.004***	-	-	-	-	-	-
$\hat{\theta}_{pre}$ x d_{tree}	-	-	-	-	2.2	***0.025***	-	-	-	-	-	-	-	-	-	-
$\hat{\theta}_{pre}$ x $\delta\theta_{pre,i}$	3.2	***0.002***	-	-	-	-	3.5	***<0.001***	-	-	-	-	1.7	*0.082*	-3.6	***<0.001***
$\delta\theta_{pre,i}$ x $\delta P_{TF,i}$	-2.0	***0.019***	-	-	-	-	-	-	-2.8	***0.004***	-	-	-	-	-	-

Hydrology and Earth System Sciences
Discussions
Open Access
EGU

https://doi.org/10.5194/hess-2022-418
Preprint. Discussion started: 6 January 2023

Hydrology and Earth System Sciences
Discussions

3.3.2 Soil water response ($\Delta\theta$)

The models for explaining the soil water content increase ($\Delta\theta$), i.e. how much water was locally stored in the soil after rain, are shown in Table 4. In general, a detectable (> 1%) change of $\Delta\theta_i$ was limited to large rainfall events (Table 1). The spatial patterns responded to several drivers (fixed effects) in the final model. There, the variance explained by fixed effects (marginal R^2) was generally higher for subsoil compared to topsoil, it typically increased with event size and was highest for the models including all event sizes (Table 4). In the following we therefore focus on the effects emerging from those latter models, that is the ones including all events, while the results for the individual event size classes are used only for more detailed interpretation. The grey shaded lines highlight the significant relations that occurred both in top- and subsoil.

Overall, local soil water content increase ($\Delta\theta$) depended not only on event median throughfall ($\hat{P}_{TF}$), but also on the spatial pattern of throughfall (δP_{TF}) and spatial patterns of initial or pre-event soil moisture ($\delta\theta_{pre}$). Nearly all main effects are also included in interactions, meaning that likely a third variable influenced the relationship between an independent and dependent variable. For example, locally elevated throughfall enhanced the soil water increase (Table 4), but more so with increasing event size (interaction $\hat{P}_{TF}$ x δP_{TF} , visualized in Figure 5 a and b).

Spatial patterns of pre-event (or initial or drained) soil water content ($\delta\theta_{pre}$) notably affected top- and subsoil differently, making it the only factor yielding opposite effects on soil water content increase in different soil depths. In topsoil, drier locations stored less water per event than moister spots (positive t-value), whereas in subsoil, the opposite was the case (negative t-value). The influence of pre-event soil moisture patterns increased with event size (interaction $\hat{P}_{TF}$ x $\delta\theta_{pre,}$). Note that the slope of the interaction (represented by the sign of the t-value) changes with overall soil water conditions consistently in both depths (Table 4, interaction $\hat{\theta}_{pre}$ x $\delta\theta_{pre,}$ visualized in Figure 6a): Locally drier soil increased soil water storage in wet, but decreased it in dry times.

Additional factors affecting the soil water response in top soil were related to the distance to the next tree. Locations near trees reacted stronger to event precipitation than those further away (interactions $\hat{P}_{TF}$ x d_{tree}), but only in overall moister soil conditions (Table 4, interaction $\hat{\theta}_{pre}$ x d_{tree}). In the subsoil higher air capacity (θ_{AC}), representing the higher macropore volume, dampened the soil water response (Table 4, negative t-value), and more so when or where throughfall was high (interactions $\hat{P}_{TF}$ x θ_{AC} and θ_{AC} x δP_{TF}) as well as in drier locations (interaction θ_{AC} x $\delta\theta_{pre}$).

https://doi.org/10.5194/hess-2022-418
Preprint. Discussion started: 6 January 2023

Table 4: Factors influencing local soil water content response after rainfall ($\Delta\theta_i$, i.e. difference between soil water content after and before each event). Results for the best linear mixed effects model including all data (left columns), and grouped according to event size (small, medium and large, right columns). Significant effects are shown in bold and factors with significant effects in both depth (based on all all events) are highlighted in grey. Variables are scaled such that the t-value indicates the effect strength. Pseudo R^2 values are given separated for fixed and random effects.

	topsoil								subsoil							
	All events		Small events		Medium events		Large event		All events		Small events		Medium events		Large events	
Full model R^2	0.57		0.10		0.32		0.54		0.62		0.38		0.46		0.55	
Fixed effects R^2	0.25		0.09		0.12		0.10		0.38		0.38		0.04		0.27	
Random effects R^2	0.32		0.01		0.20		0.43		0.24		0.00		0.42		0.28	
	t-value	p-value	t-value	p-value	t-value	p-value	t-value	p-value	t-value	p-value	t-value	p-value	t-value	p-value	t-value	p-value
Fixed effects																
Median event throughfall, $\hat{P}_{TF}$	***5.1***	***<0.001***	-	-	***3.5***	***0.014***	1.3	0.215	***6.8***	***<0.001***	***3.4***	***<0.001***	-	-	***4.1***	***0.001***
Spatial throughfall pattern, $\delta P_{TF,i}$	***2.0***	***0.044***	-	-	***2.2***	***0.030***	***2.2***	***0.031***	***3.0***	***0.003***	-	-	-	-	***3.3***	***<0.001***
Initial median soil water content, $\hat{\theta}_{pre}$	0.4	0.712	***5.6***	***<0.001***	1.3	0.241	0.9	0.382	-0.3	0.787	***-10.9***	***<0.001***	-	-	0.2	0.843
Spatial pattern of initial soil water content, $\delta\theta_{pre,i}$	***4.2***	***<0.001***	-	-	-	-	***3.3***	***0.001***	***-3.9***	***<0.001***	***-2.4***	***0.017***	-	-	***-4.3***	***<0.001***
Tree Distance, d_{tree}	1.3	0.211	-	-	***2.9***	***0.004***	0.6	0.569	-	-	-	-	1.5	0.144	-	-
Air capacity, $\theta_{AC,i}$	-	-	-	-	-0.8	0.398	-	-	***-2.4***	***0.016***	-1.4	0.173	-1.0	0.337	***-2.8***	***0.007***
Interactions																
$\hat{P}_{TF}$ x $\delta P_{TF,i}$	***2.4***	***0.016***	-	-	-	-	-	-	***3.7***	***<0.001***	-	-	-	-	-	-
$\hat{P}_{TF}$ x $d_{tree,i}$	***-2.3***	***0.020***	-	-	-	-	***-2.8***	***0.005***	-	-	-	-	***2.5***	***0.012***	-	-
$\hat{P}_{TF}$ x $\hat{\theta}_{pre}$	-	-	-	-	-	-	-	-	-	-	-	-	-	-	-	-
$\hat{P}_{TF}$ x $\delta\theta_{pre,i}$	***4.5***	***<0.001***	-	-	-	-	-	-	***-5.3***	***<0.001***	***3.3***	***<0.001***	-	-	***-3.3***	***<0.001***
$\hat{P}_{TF}$ x $\theta_{AC,i}$					***-2.9***	***0.003***			***-3.3***	***0.001***	***2.6***	***0.011***	***2.6***	***0.009***	-	-
$\theta_{AC,i}$ x $\delta P_{TF,i}$	-	-	-	-	-	-	-	-	***-4.0***	***<0.001***	-	-	-	-	***-3.8***	***<0.001***
$\theta_{AC,i}$ x d_{tree}	-	-	-	-	***-2.6***	***0.012***	-	-	-	-	-	-	1.9	0.061	-	-
$\theta_{AC,i}$ x $\delta\theta_{pre,i}$	-	-	-	-	-	-	-	-	***3.7***	***<0.001***	-	-	-	-	***3.5***	***<0.001***
$\hat{\theta}_{pre}$ x $\delta P_{TF,i}$	-	-	-	-	***2.1***	***0.034***	***-2.1***	***0.033***	-	-	-	-	-	-	-	-
$\hat{\theta}_{pre}$ x d_{tree}	***2.1***	***0.032***	-	-	***2.4***	***0.018***	-	-	-	-	-	-	-	-	-	-
$\hat{\theta}_{pre}$ x $\delta\theta_{pre,i}$	***-6.5***	***<0.001***	-	-	-	-	***-7.3***	***<0.001***	***-2.5***	***0.011***	***-2.3***	***0.020***	-	-	***-2.6***	***0.011***
$\delta\theta_{pre,i}$ x $\delta P_{TF,i}$	-	-	-	-	-	-	-	-	***-2.4***	***0.016***	-	-	-	-	***-2.0***	***0.048***

Hydrology and Earth System Sciences
Discussions
Open Access
EGU

https://doi.org/10.5194/hess-2022-418
Preprint. Discussion started: 6 January 2023

Hydrology and Earth System Sciences
Discussions
Open Access
EGU

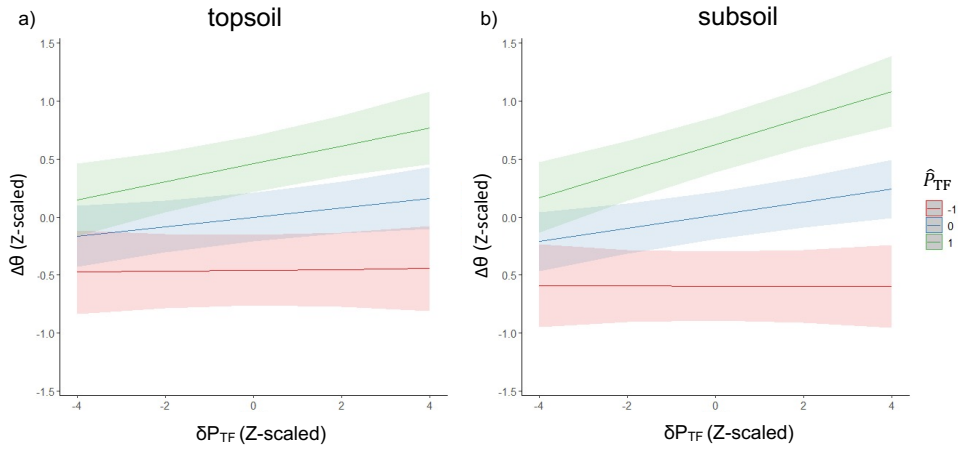

Fig. 5: Influence of the spatial pattern of throughfall (δP_{TF}) and on the soil water content response ($\Delta\theta$), grouped by the event size (given as mean of throughfall, $\hat{P}_{TF}$) for (**left**) topsoil and (**right**) subsoil. Note that all values are z-scaled, and therefore centered around zero. For example, the red line highlights events of below average throughfall (small events). There, the spatial pattern of soil water content response depends little on that of throughfall (small events). A stronger influence is seen for the above average (larger) events marked in green.

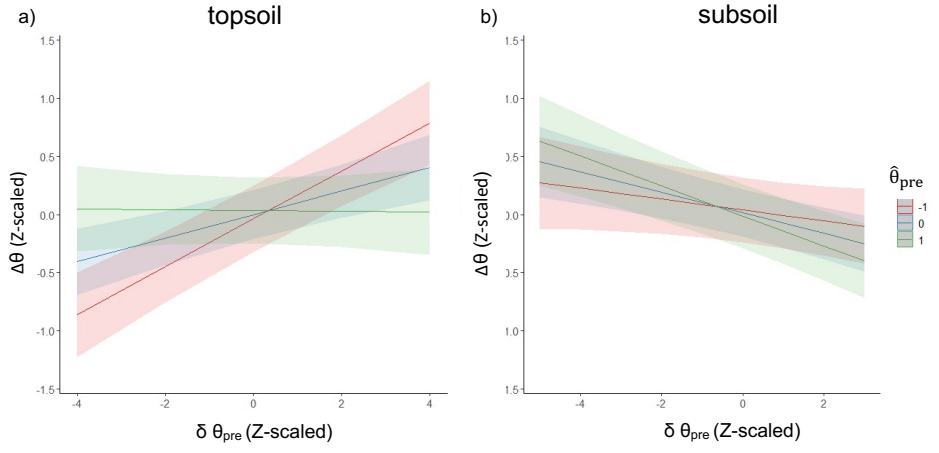

Fig 6. Interaction between the local soil water response to rain event ($\Delta\theta$) and the local pre-event soil water content pattern ($\delta\theta_{pre}$) grouped by the pre-event spatial average soil moisture conditions (spatial median soil water content, $\hat{\theta}_{pre}$) for (**left**) topsoil and (**right**) subsoil. For example, the green line shows that in overall moist conditions (e.g. early spring), soil water content increase is dampened in moister locations (high values of $\delta\theta_{pre}$) and more so on the subsoil. Dampening also takes place in drier locations in dry summer conditions in topsoil (red line). Note: grouping according to soil water content ($\hat{\theta}_{pre}$) was done separately for topsoil and subsoil, while absolute values in subsoil water content are always higher than in topsoil. Therefore, the shift in slopes from positive to negative with soil moisture conditions is not only within but also between soil depth.

https://doi.org/10.5194/hess-2022-418
Preprint. Discussion started: 6 January 2023

Hydrology and Earth System Sciences
Discussions

4. Discussion

4.1 Strengths and weaknesses of the approach

In this analysis we used extensive spatial data of canopy cover, throughfall and soil water content in order to assess the role of canopy processes on below-ground soil water response to precipitation. For this, we meassured precipitation and soil water content at different locations in order to avoid disturbance of soil water dynamics by the precipitation measurement and providing independent random measurement designs. To be able to relate observations at different locations, we used geostatistical methods to predict throughfall values at locations where soil water content was measured. Because the throughfall prediction can be based on an extensive dataset of 350 points, it allows reliable variogram estimations (Voss et al., 2016). Throughfall showed strong spatial autocorrelation which was reflected by nugget-to-still ratios much lower than 25% for all event sizes (Table S3). However, spatial correlation patterns depended on event size in that the correlation length decreased with increasing event rainfall. This decreased in larger events the range within which throughfall could be predicted and increased the number of locations with high kriging variance, that were removed from the analysis. As a result, this decreased the sample size for large compared to small and medium sized events. Regardless, for all sampled events, we could still rely on datasets of 59 points on average. Additionally, kriging predictions tend to be smoother compared to the actual data. However, the predicted values show approximately the same median and spatial variance as the measured data, indicating that the real variation was still maintained after the prediction procedure. Unfortunately, there is no perfect way to relate measurements obtained at different locations to each other. However, the combination of a large sample size of throughfall and variogram estimation by residual maximum likelihood (REML) seems to be a suitable way forward for interpolating the aboveground data to the belowground locations (Lark, 2000; Voss et al., 2016). Altogether, this provides a good basis to comparing above- and belowground measurements.

In our analysis we quantified only throughfall input and omit the role of stemflow, which may play a role in locations near stems. Extrapolating stemflow input to soil moisture locations entails more prediction steps compared to throughfall. Spatial variation of stemflow depends on the one hand on species, tree and canopy size, neighborhood and individual morphology of the trees (Bellot and Escarre, 1998; Fan et al., 2015b; Levia et al., 2014; Levia and Germer, 2015; Van Stan et al., 2016; Metzger et al., 2019; Magliano et al., 2019) and on the other hand on precipitation intensity and soil conditions determining the infiltration area (Herwitz, 1986; Carlyle-Moses et al., 2018; Metzger et al., 2021). Such a prediction would not only introduce a great deal of uncertainty, but also deviate from the main purpose of this study, which is to evaluate the role of throughfall heterogeneity. Therefore, in the model analysis, microsites near stems were accounted for by including distance to the stem as fixed effect in the model. This takes into account to some extent the potential influence of stemflow in the interpretation.

4.2 General patterns of throughfall (temporal and spatial)

In agreement with previous studies, throughfall patterns of large events show lower coefficients of variation compared to smaller ones (Aussenac, 1970; Loustau et al., 1992; Llorens et al., 1997; Su et al., 2019; Metzger et al., 2017; Carlyle-Moses, 2004; Staelens et al., 2008; Van Stan et al., 2020). Several other studies have suggested that throughfall spatial variation depend next to canopy characteristics also on precipitation amount (Loustau et al., 1992; Carlyle-Moses, 2004; Keim et al., 2005; Park and Cameron, 2008; Hsueh et al., 2016; Zimmermann et al., 2009). Similarly, at our site for all event size classes, canopy cover was a significant driver of throughfall spatial distribution, although a small one compared to the random effects. The correlation length (effective range) of throughfall decreased with increasing event size and corresponded for medium events roughly to that of canopy

https://doi.org/10.5194/hess-2022-418
Preprint. Discussion started: 6 January 2023

cover. The change of spatial pattern with event size illustrates that not only canopy storage per se, but also other processes like turbulence, wind shadows, the arrangement of canopy gaps, or the formation of canopy dripping points can add persistent spatial organization to below-canopy precipitation (Carlyle-Moses, 2004; Keim et al., 2005; Park and Cameron, 2008; Staelens et al., 2008; Zimmermann et al., 2008; Wullaert et al., 2009; Li et al., 2016; Van Stan et al., 2020). In other words, not only canopy density, but also other canopy features probably affect throughfall distribution (Park and Cameron, 2008; Zimmermann et al., 2009). Overall, and despite the slight changes in throughfall correlation lengths for different events size classes, throughfall patterns were temporally stable, indicating the existence of permanent hot and cold spots of throughfall, and those were consistent across small, medium and large events. This is in line with several previous studies stating temporal stability of throughfall patterns (Keim et al., 2005; Staelens et al., 2006; Wullaert et al., 2009; Zimmermann et al., 2009; Fathizadeh et al., 2014; Fan et al., 2015b; Metzger et al., 2017; Molina et al., 2019; Zhu et al., 2021; Rodrigues et al., 2022) even over several years (Wullaert et al., 2009; Rodrigues et al., 2022), although phenology and canopy development have also been observed to deteriorate spatial stability (Zimmermann et al., 2008; Fathizadeh et al., 2014). Furthermore, although spatial variation coefficients are smaller in large compared to small events, absolute values vary much more in large events such that they have arguably a higher potential to induce spatial patterns in soil water content or dynamics.

4.3 General soil water content patterns and potential drivers

Mean soil water contents were generally lower in the topsoil compared to the subsoil. At our site, the shallow soil is underlain by undulating weathered calcareous bedrock (Kohlhepp et al., 2017) of low hydraulic conductivity, and may locally be broken through by tree roots. While the topsoil is well-drained (i.e. saturated to field capacity in winter and much lower in summer), the deeper and finer textured soil layer (Metzger et al., 2021) is influenced by the much less conductive regolith and generally moister soil water content which very occasionally exceeds field capacity in winter (Metzger et al., 2017).

Much in agreement with previous studies in humid regions (Brocca et al., 2007; Korres et al., 2015; Rosenbaum et al., 2012; Metzger et al., 2017), spatial variation of soil water content increased in both top- and subsoil in drier summer soil conditions. In an earlier study at the same site a strong but short-lived increase of spatial variation of topsoil water content in summer was related to precipitation events (Metzger et al., 2017). Regardless, we found that the main controlling factor of post-event soil water content was the spatial pattern of pre-event soil water content, while average throughfall and spatial pattern of throughfall, tree distance and air capacity were additional, but much less important drivers. In other words, while soil water content variation increases strongly after events, this variation can only in very limited fashion be traced back to input patterns. This may in part be due to the small inputs of water compared to the overall soil water storage, leading to a strong memory effect of the pre-event soil water conditions on the post event patterns. Furthermore, preferential flow already taking place during the event itself can blur the throughfall pattern within the soil storage (see below).

Soil water content spatial patterns in drained state in turn were strongly driven by random effects. Those are factors that were not described by the measurements, but are temporally stable. Those so called local soil conditions are potentially related to soil hydraulic properties, root water uptake and microtopography (Famiglietti et al., 1998; Vereecken et al., 2007; Fan et al., 2015a). The mixed-effects models confirm, although with a very week influence, that locations of higher air capacity (higher macroporosity) were drier in both depths, confirming the role of water retention on soil water patterns (Metzger et al., 2017) at this site. Also, throughfall patterns of the previous event

https://doi.org/10.5194/hess-2022-418
Preprint. Discussion started: 6 January 2023

slightly affected topsoil pre-event soil water content. Thus, an imprint of the throughfall pattern was carried over to the next pre-event soil conditions, but this is barely detectable and negligible compared to the other sources of variation in soil water content in drained state.

4.4 Drivers of soil water response ($\Delta\theta$) to rainfall

In contrast to the absolute values of soil water contents discussed above, the local soil water response (i.e. increase of soil water content following rainfall events), was clearly driven by the spatial throughfall pattern both in top- and subsoil. Since we tested the effect of the spatial pattern (δP_{TF}) separately from the absolute values of event throughfall ($\hat{P}_{TF}$), we are able to demonstrate the influence of spatial throughfall specifically. Among all drivers tested, the influence of spatial throughfall variation was the most consistent, appeared in both observed soil depths, and was more pronounced for larger events. In other words, spatial patterns of throughfall were the most prominent driver of soil wetting.

Measurements ascertaining that soil water content response relates to canopy drainage are comparatively rare. Metzger et al. (2017) already reported for the same site, but a smaller dataset, that soil water content increase correlated with event spatial throughfall patterns in larger rainfall events. Molina et al., (2019) found with highly temporally resolved soil moisture measurements a weak relationship between the average pattern of throughfall and that of soil water content response in the topsoil of a Mediterranean oak dominated forest plot, but not in a pine plot. Notably, Klos et al. (2014) in a tropical rain forests showed that locations of high and low soil water content below the main rooting zone corresponded to the end members of high and low throughfall, while soil water content was more homogenous above and below this depth. They concluded from additional modelling that preferential flow may have contributed to bypassing the main rooting zone. On the other hand, several studies, such as Raat et al. (2002), Shachnovich and Berliner, (2008), and more recently Zhu et al. (2021) with temporally less highly resolved soil water content measurements (incidentally all in coniferous forests) did not find relations between the spatial patterns of soil water content and throughfall. All authors report that throughfall patterns were pronounced and stable in time and suspect the forests floor hindered the transmission to soil water patterns. An additional explanation could be that the effect of spatial net precipitation patterns on soil water content were so short-lived (Metzger et al., 2017) due to preferential flow that they were not observed by infrequent hand measurements. Altogether stronger soil water response at locations with above average throughfall indicates that throughfall hot spots and also cold spots (Levia and Frost, 2006; Van Stan et al., 2020; Zimmermann et al., 2009) translated into soil water dynamics, despite them going almost unnoticed in the soil water content pattern (see above).

Next to the throughfall pattern, soil water response after large rainfall events depended in both depths also on the pattern of pre-event soil water content. Notably, the slope of the relationship changes direction, making it the only factor that shows opposite effects in the top- and subsoil. This can be attributed to its inter-dependence on soil water content, and the difference in moisture between the two measurement depths. Especially in dry (summer) conditions, wetter topsoil locations took up more of the arriving precipitation water, whereas drier locations remained dry. This is a strong indication of preferential flow in dry soil, where e.g. hydrophobic conditions, cracks and low hydraulic conductivity of the matrix can enhance preferential flow (Hillel, 1998; Nimmo, 2021; Beven and Germann, 2013). On the other hand, the dampened water response in the wetter subsoil, could be due to enhanced hydraulic conductivity and less free pore space (Vereecken et al., 2007; Hagen et al., 2020). Only in

https://doi.org/10.5194/hess-2022-418
Preprint. Discussion started: 6 January 2023


Hydrology and Earth System Sciences
Discussions
Open Access
EGU

intermediate soil water contents the spatial distribution of soil water contents had no influence on the spatial drainage behavior.

Soil water response depended additionally also on the distance to the nearest tree in the topsoil and soil properties (air capacity) in the subsoil. The enhanced moistening of soils near stems is likely related to stemflow production (Metzger et al., 2019), which was not accounted for as input. Stemflow production generally increases with event size (Levia and Germer, 2015; Metzger et al., 2019), explaining the interaction in the model. The additional modification by soil water conditions can be explained by the systematically lower soil water contents near tree trunks at the same site (Metzger et al., 2017, 2021), due to lower soil water retention and likely enhanced drainage there.

Taken together, our data strongly suggest that additionally to spatial distribution of throughfall, the spatial pattern in drainage behavior affects the local soil water response to rainfall. In that, both dry and wet locations can, water supply permitting, act as percolation hotspots, depending on the overall soil conditions. Bypass flow in forests has been repeatedly observed (e.g. Schume et al., 2003; Schwärzel et al., 2009; Bachmair et al., 2012; Blume et al., 2009; Demand et al., 2019) especially in dry summer conditions (Schume et al., 2003; Bachmair et al., 2012; Demand et al., 2019). Spatial variation of infiltration water supply and intensity, such as is the case for below canopy precipitation (Keim and Link, 2018), has been suggested as a potential cause for initiating finger flow (Nimmo, 2021), which is promoted by dry soil conditions. Also, hydrophobicity has been suggested to contribute to maintaining recurring finger flow paths (Blume et al., 2009). Next to this, macropore flow along biopores (Lange et al., 2009; Nespoulous et al., 2019) and soil cracks (Schume et al., 2003) can be enhanced in dry forest soil conditions due to soil shrinking (Baram et al., 2012). While both finger flow and macropore flow may have contributed to the observed patterns in soil water response, macropore flow more than finger flow could explain enhanced matter export (Lehmann et al., 2021) as well as fast response following strong storms observed in the shallow aquifers of the AquaDiva Critical Zone Observatory (Lehmann and Totsche, 2020).

Overall, our results confirm that the effect of throughfall on soil water content is weak, but stronger on the soil water response. This contrasts with previous modelling (Coenders-Gerrits et al., 2013) that did not account for preferential flow. With the effect of the throughfall pattern on the soil water response also depending on local conditions related to hydraulic properties, its fate is much more likely to be found in the drainage fluxes, next to the storage. The further destiny of the net precipitation pattern arguably depends on the deeper subsurface hydrogeological setting. We deduce however, that net precipitation hotspots have a strong chance of producing patterns of preferential flow below the main rooting zone, which is in line with previous work (Klos et al., 2014), and backs earlier hypotheses (Bouten et al., 1992; Schume et al., 2003).

5. Conclusion

In this study, we collected an extensive dataset to investigate the effect of throughfall spatial heterogeneity on the soil water response and checked which other factors (pre-event soil water content, macroporosity, tree distance) modified the result. We first confirmed that throughfall patterns were stable in time and found that they related to the vegetation canopy density, although additional and partly unknown factors strongly affected throughfall distribution. We found that post event soil water content per se did have a very weak relation to throughfall, although the variation of soil water content clearly increased in the aftermath of rain events. The post-event soil water content pattern was overwhelmingly determined by the strong memory effect of the soil water storage and only slightly affected by soil properties, like macroporosity. In contrast, the soil water response showed a clear relation with the throughfall input pattern. In other words, our setup allowed us to

https://doi.org/10.5194/hess-2022-418
Preprint. Discussion started: 6 January 2023

confirm experimentally that throughfall patterns do imprint on soil water content dynamics, at least shortly after rain events. However, we also identified locations where soil water response was dampened, likely due to enhanced fast drainage. Those locations could be either very dry locations likely promoting preferential flow, especially in the topsoil, or wet locations, promoting faster release of the incoming water. Our results demonstrate that throughfall spatial patterns leave a stronger imprint on soil water dynamics than on soil water content directly, and explain why aboveground influence on soil hydrology has been so difficult to lay open in the past. Our results are in line with previous research and contribute a more general process understanding of the below ground consequences of precipitation redistribution by forests. Most importantly, our results strongly suggest that throughfall patterns induce fast soil water flow with repeating spatial patterns. Those patterns would therefore already be triggered within the canopy.

Acknowledgements

We thank Murray Lark for insightful comments on the strategy for comparing above and belowground spatial patterns that helped shaping the geostatistical analysis.

This study is part of the Collaborative Research Centre AquaDiva of the Friedrich Schiller University Jena, funded by the Deutsche Forschungsgemeinschaft (DFG, German Research Foundation) – SFB 1076 – Project Number 218627073. We thank the Hainich CZE site manager Robert Lehmann and the Hainich National Park. Field work permits were issued by the responsible state environmental offices of Thüringen.

Data availability

The dataset is currently prepared for publishing in a official repository. The doi will be posted with the data at the latest when the data is published.

Author contributions

AH developed the project idea. All authors contributed to the collection of the raw data. CF conducted the statistical analysis, developed it further with AH, and both wrote the first draft of the manuscript. All authors contributed to writing of the manuscript.

6. References

Aussenac, G.: Action du couvert forestier sur la distribution au sol des précipitations, Annales des Sciences Forestières, 27, 383–399, https://doi.org/10.1051/forest/19700403, 1970.

Bachmair, S., Weiler, M., and Troch, P. A.: Intercomparing hillslope hydrological dynamics: Spatio-temporal variability and vegetation cover effects, Water Resources Research, 48, 1–18, https://doi.org/10.1029/2011WR011196, 2012.

Baram, S., Kurtzman, D., and Dahan, O.: Water percolation through a clayey vadose zone, Journal of Hydrology, 424–425, 165–171, https://doi.org/10.1016/j.jhydrol.2011.12.040, 2012.

Barton, K.: MuMIn: Multi-Model Inference, 2020.

Bates, D., Mächler, M., Bolker, B., and Walker, S.: Fitting Linear Mixed-Effects Models Using lme4, Journal of Statistical Software, 67, 1–48, https://doi.org/10.18637/jss.v067.i01, 2015.

Bellot, J. and Escarre, A.: Stemflow and throughfall determination in a resprouted Mediterranean holm-oak forest, Annales des Sciences Forestières, 55, 847–865, https://doi.org/10.1051/forest:19980708, 1998.

https://doi.org/10.5194/hess-2022-418
Preprint. Discussion started: 6 January 2023

609 Beven, K. and Germann, P.: Macropores and water flow in soils revisited, Water Resources Research, accepted,
610 https://doi.org/10.1002/wrcr.20156, 2013.
611 Blume, T., Zehe, E., and Bronstert, a.: Use of soil moisture dynamics and patterns at different spatio-temporal
612 scales for the investigation of subsurface flow processes, Hydrology and Earth System Sciences, 13,
613 1215–1233, https://doi.org/10.5194/hess-13-1215-2009, 2009.
614 Bogena, H. R., Herbst, M., Huisman, J. A., Rosenbaum, U., Weuthen, A., and Vereecken, H.: Potential of
615 Wireless Sensor Networks for Measuring Soil Water Content Variability, Vadoze Zone Journal, 9, 1002–
616 1013, https://doi.org/10.2136/vzj2009.0173, 2010.
617 Bouten, W., Heimovaara, T. J., and Tiktak, A.: Spatial patterns of throughfall and soil water dynamics in a
618 Douglas fir stand, Water Resources Research, 28, 3227–3233, https://doi.org/10.1029/92WR01764, 1992.
619 Brocca, L., Morbidelli, R., Melone, F., and Moramarco, T.: Soil moisture spatial variability in experimental
620 areas of central Italy, Journal of Hydrology, 333, 356–373, https://doi.org/10.1016/j.jhydrol.2006.09.004,
621 2007.
622 Brown, A. E., Zhang, L., McMahon, T. A., Western, A. W., and Vertessy, R. A.: A review of paired catchment
623 studies for determining changes in water yield resulting from alterations in vegetation, Journal of
624 Hydrology, 310, 28–61, https://doi.org/10.1016/j.jhydrol.2004.12.010, 2005.
625 Carlyle-Moses, D. E.: Throughfall, stemflow, and canopy interception loss fluxes in a semi-arid Sierra Madre
626 Oriental matorral community, Journal of Arid Environments, 58, 181–202, https://doi.org/10.1016/S0140-
627 1963(03)00125-3, 2004.
628 Carlyle-Moses, D. E. and Gash, J. H. C.: Rainfall Interception Loss by Forest Canopies, in: Forest Hydrology
629 and Biogeochemistry: Synthesis of Past Research and Future Directions, Ecological Studies 216, edited
630 by: Levia, D. F., Carlyle-Moses, D. E., and Tanaka, T., Spinger Science+Buisness Media, 407–423,
631 https://doi.org/10.1007/978-94-007-1363-5, 2011.
632 Carlyle-Moses, D. E., Iida, S., Germer, S., Llorens, P., Michalzik, B., Nanko, K., Tischer, A., and Levia, D. F.:
633 Expressing stemflow commensurate with its ecohydrological importance, Advances in Water Resources,
634 121, 472–479, https://doi.org/10.1016/j.advwatres.2018.08.015, 2018.
635 Coenders-Gerrits, A. M. J., Hopp, L., Savenije, H. H. G., and Pfister, L.: The effect of spatial throughfall
636 patterns on soil moisture patterns at the hillslope scale, Hydrology and Earth System Sciences, 17, 1749–
637 1763, https://doi.org/10.5194/hess-17-1749-2013, 2013.
638 Cressie, N. and Hawkins, D. M.: Robust estimation of the variogram: I, Mathematical Geology, 12, 115–125,
639 https://doi.org/10.1007/BF01035243, 1980.
640 Demand, D., Blume, T., and Weiler, M.: Spatio-temporal relevance and controls of preferential flow at the
641 landscape scale, Hydrology and Earth System Sciences, 23, 4869–4889, https://doi.org/10.5194/hess-23-
642 4869-2019, 2019.
643 Dowd, P. A.: The Variogram and Kriging: Robust and Resistant Estimators, in: Geostatistics for Natural
644 Resources Characterization: Part 1, edited by: Verly, G., David, M., Journel, A. G., and Marechal, A.,
645 Springer Netherlands, Dordrecht, 91–106, https://doi.org/10.1007/978-94-009-3699-7_6, 1984.
646 Durocher, M. G.: Monitoring spatial variability of forest interception, Hydrological Processes, 4, 215–229, 1990.
647 Falkengren-Grerup, U.: Effect of stemflow on beech forest soils and vegetation in southern Sweden, Plant
648 Ecology, 26, 341–352, 1989.
649 Famiglietti, J. S., Rudnicki, J. W., and Rodell, M.: Variability in surface moisture content along a hillslope
650 transect: Rattlesnake Hill, Texas, Journal of Hydrology, 210, 259–281, https://doi.org/10.1016/S0022-
651 1694(98)00187-5, 1998.
652 Fan, J., Scheuermann, A., Guyot, A., Baumgartl, T., and Lockington, D. A.: Quantifying spatiotemporal
653 dynamics of root-zone soil water in a mixed forest on subtropical coastal sand dune using surface ERT
654 and spatial TDR, Journal of Hydrology, 523, 475–488, https://doi.org/10.1016/j.jhydrol.2015.01.064,
655 2015a.
656 Fan, J., Oestergaard, K. T., Guyot, A., Jensen, D. G., and Lockington, D. A.: Spatial variability of throughfall
657 and stemflow in an exotic pine plantation of subtropical coastal Australia, Hydrological Processes, 29,
658 793–804, https://doi.org/10.1002/hyp.10193, 2015b.
659 Fathizadeh, O., Attarod, P., Keim, R. F., Stein, A., Amiri, G. Z., and Darvishsefat, A. A.: Spatial heterogeneity
660 and temporal stability of throughfall under individual Quercus brantii trees, Hydrological Processes, 28,
661 1124–1136, https://doi.org/10.1002/hyp.9638, 2014.
662 Genton, M. G.: Highly Robust Variogram Estimation, Mathematical Geology, 30, 213–221,
663 https://doi.org/10.1023/A:1021728614555, 1998.
664 Germer, S.: Development of near-surface perched water tables during natural and artificial stemflow generation
665 by babassu palms, Journal of Hydrology, 507, 262–272, https://doi.org/10.1016/j.jhydrol.2013.10.026,
666 2013.
667 Gerrits, A. M. J. and Savenije, H. H. G.: Forest Floor Interception, in: Forest Hydrology and Biogeochemistry:
668 Synthesis of Past Research and Future Directions, edited by: Levia, D. F., Carlyle-Moses, D., and Tanaka,
669 T., Springer Netherlands, Dordrecht, 445–454, https://doi.org/10.1007/978-94-007-1363-5_22, 2011.
670 Gräler, B., Pebesma, E., and Heuvelink, G.: Spatio-Temporal Interpolation using gstat, The R Journal, 8, 204–

https://doi.org/10.5194/hess-2022-418
Preprint. Discussion started: 6 January 2023

218, 2016.
Guswa, A. J.: Canopy vs. Roots: Production and Destruction of Variability in Soil Moisture and Hydrologic Fluxes, Vadose Zone Journal, 11, https://doi.org/10.2136/vzj2011.0159, 2012.
Guswa, A. J. and Spence, C. M.: Effect of throughfall variability on recharge: Application to hemlock and deciduous forests in western Massachusetts, Ecohydrology, 5, 563–574, https://doi.org/10.1002/eco.281, 2012.
Guswa, A. J., Tetzlaff, D., Selker, J. S., Carlyle-Moses, D. E., Boyer, E. W., Bruen, M., Cayuela, C., Creed, I. F., van de Giesen, N., Grasso, D., Hannah, D. M., Hudson, J. E., Hudson, S. A., Iida, S., Jackson, R. B., Katul, G. G., Kumagai, T., Llorens, P., Lopes Ribeiro, F., Michalzik, B., Nanko, K., Oster, C., Pataki, D. E., Peters, C. A., Rinaldo, A., Sanchez Carretero, D., Trifunovic, B., Zalewski, M., Haagsma, M., and Levia, D. F.: Advancing ecohydrology in the 21st century: A convergence of opportunities, Ecohydrology, 13, 1–14, https://doi.org/10.1002/eco.2208, 2020.
Hagen, K., Berger, A., Gartner, K., Geitner, C., Kofler, T., Kogelbauer, I., Kohl, B., Markart, G., Meißl, G., and Niedertscheider, K.: Event-based dynamics of the soil water content at Alpine sites (Tyrol, Austria), Catena, 194, https://doi.org/10.1016/j.catena.2020.104682, 2020.
Herwitz, S. R.: Infiltration-excess caused by Stemflow in a cyclone-prone tropical rainforest, Earth Surf. Process. Landforms, 11, 401–412, https://doi.org/10.1002/esp.3290110406, 1986.
Hillel, D.: Environmental Soil Physics, Academic Press, Boston, 771 pp., 1998.
Horton, R. E.: Rainfall Interception, Monthly Weather Review, 47, 603–623, https://doi.org/10.1175/1520-0493(1919)47<603:RI>2.0.CO;2, 1919.
Hsueh, Y. H., Allen, S. T., and Keim, R. F.: Fine-scale spatial variability of throughfall amount and isotopic composition under a hardwood forest canopy, Hydrological Processes, 30, 1796–1803, https://doi.org/10.1002/hyp.10772, 2016.
Keim, R., Skaugset, a, and Weiler, M.: Temporal persistence of spatial patterns in throughfall, Journal of Hydrology, 314, 263–274, https://doi.org/10.1016/j.jhydrol.2005.03.021, 2005.
Keim, R. F. and Link, T. E.: Linked spatial variability of throughfall amount and intensity during rainfall in a coniferous forest, Agricultural and Forest Meteorology, 248, 15–21, https://doi.org/10.1016/j.agrformet.2017.09.006, 2018.
Kimmins, J. P.: Some Statistical Aspects of Sampling Throughfall Precipitation in Nutrient Cycling Studies in British Columbian Coastal Forests, Ecology, 54, 1008–1019, https://doi.org/10.2307/1935567, 1973.
Klos, P. Z., Chain-Guadarrama, A., Link, T. E., Finegan, B., Vierling, L. A., and Chazdon, R.: Throughfall heterogeneity in tropical forested landscapes as a focal mechanism for deep percolation, Journal of Hydrology, 519, 2180–2188, https://doi.org/10.1016/j.jhydrol.2014.10.004, 2014.
Kohlhepp, B., Lehmann, R., Seeber, P., Küsel, K., Trumbore, S. E., and Totsche, K. U.: Aquifer configuration and geostructural links control the groundwater quality in thin-bedded carbonate-siliciclastic alternations of the Hainich CZE, central Germany, Hydrology and Earth System Sciences, 21, 6091–6116, https://doi.org/10.5194/hess-21-6091-2017, 2017.
Korres, W., Reichenau, T. G., Fiener, P., Koyama, C. N., Bogena, H. R., Cornelissen, T., Baatz, R., Herbst, M., Diekkrüger, B., Vereecken, H., and Schneider, K.: Spatio-temporal soil moisture patterns – A meta-analysis using plot to catchment scale data, Journal of Hydrology, 520, 326–341, https://doi.org/10.1016/j.jhydrol.2014.11.042, 2015.
Küsel, K., Totsche, K. U., Trumbore, S. E., Lehmann, R., Steinhäuser, C., and Herrmann, M.: How Deep Can Surface Signals Be Traced in the Critical Zone? Merging Biodiversity with Biogeochemistry Research in a Central German Muschelkalk Landscape, Frontiers in Earth Science, 4, 1–18, https://doi.org/10.3389/feart.2016.00032, 2016.
Kuznetsova, A., Brockhoff, P. B., and Christensen, R. H. B.: lmerTest Package: Tests in Linear Mixed Effects Models, Journal of Statistical Software, 82, 1–26, https://doi.org/10.18637/jss.v082.i13, 2017.
Lange, B., Lüescher, P., and Germann, P. F.: Significance of tree roots for preferential infiltration in stagnic soils, Hydrology and Earth System Sciences, 13, 1809–1821, https://doi.org/10.5194/hess-13-1809-2009, 2009.
Lark, R. M.: A comparison of some robust estimators of the variogram for use in soil survey, European Journal of Soil Science, 51, 137–157, https://doi.org/10.1046/j.1365-2389.2000.00280.x, 2000.
Lehmann, K., Lehmann, R., and Totsche, K. U.: Event-driven dynamics of the total mobile inventory in undisturbed soil account for significant fluxes of particulate organic carbon, Science of the Total Environment, 756, 143774, https://doi.org/10.1016/j.scitotenv.2020.143774, 2021.
Lehmann, R. and Totsche, K. U.: Multi-directional flow dynamics shape groundwater quality in sloping bedrock strata, Journal of Hydrology, 580, 124291, https://doi.org/10.1016/j.jhydrol.2019.124291, 2020.
Levia, D. F. and Frost, E. E.: Variability of throughfall volume and solute inputs in wooded ecosystems, Progress in Physical Geography: Earth and Environment, 30, 605–632, https://doi.org/10.1177/0309133306071145, 2006.
Levia, D. F. and Germer, S.: A review of stemflow generation dynamics and stemflow-environment interactions in forests and shrublands, Reviews of Geophysics, 53, 673–714,

https://doi.org/10.5194/hess-2022-418
Preprint. Discussion started: 6 January 2023

Hydrology and Earth System Sciences
Discussions
Open Access
EGU

https://doi.org/10.1002/2015RG000479.Received, 2015.
Levia, D. F., Michalzik, B., Näthe, K., Bischoff, S., Richter, S., and Legates, D. R.: Differential stemflow yield from European beech saplings: The role of individual canopy structure metrics, Hydrological Processes, https://doi.org/10.1002/hyp.10124, 2014.
Li, X., Xiao, Q., Niu, J., Dymond, S., van Doorn, N. S., Yu, X., Xie, B., Lv, X., Zhang, K., and Li, J.: Process-based rainfall interception by small trees in Northern China: The effect of rainfall traits and crown structure characteristics, Agricultural and Forest Meteorology, 218–219, 65–73, https://doi.org/10.1016/j.agrformet.2015.11.017, 2016.
Liang, W. L., Li, S. L., and Hung, F. X.: Analysis of the contributions of topographic, soil, and vegetation features on the spatial distributions of surface soil moisture in a steep natural forested headwater catchment, Hydrological Processes, 31, 3796–3809, https://doi.org/10.1002/hyp.11290, 2017.
Liang, W.-L., Kosugi, K., and Mizuyama, T.: Heterogeneous Soil Water Dynamics around a Tree Growing on a Steep Hillslope, Vadose Zone Journal, 6, 879–889, https://doi.org/10.2136/vzj2007.0029, 2007.
Llorens, P., Poch, R., Latron, J., and Gallart, F.: Rainfall interception by a Pinus sylvestris forest patch overgrown in a Mediterranean mountainous abandoned area I. Monitoring design and results down to the event scale, Journal of Hydrology, 199, 331–345, https://doi.org/10.1016/S0022-1694(96)03334-3, 1997.
Lloyd, C. R. and Marques, A. D. O.: Spatial variability of throughfall and stemflow measurements in Amazonian rainforest, Agricultural and Forest Meteorology, 42, 63–73, https://doi.org/10.1016/0168-1923(88)90067-6, 1988.
Loustau, D., Berbigier, P., and Granier, a.: Interception loss, throughfall and stemflow in a maritime pine stand. II. An application of Gash's analytical model of interception, Journal of Hydrology, 138, 469–485, https://doi.org/10.1016/0022-1694(92)90131-E, 1992.
Magliano, P. N., Whitworth-Hulse, J. I., Florio, E. L., Aguirre, E. C., and Blanco, L. J.: Interception loss, throughfall and stemflow by *Larrea divaricata* : The role of rainfall characteristics and plant morphological attributes, Ecological Research, 34, 753–764, https://doi.org/10.1111/1440-1703.12036, 2019.
Matheron, G.: Traité de géostatistique appliquée, Éditions Technip, Paris, 333 pp., 1962.
Metzger, J. C., Wutzler, T., Dalla Valle, N., Filipzik, J., Grauer, C., Lehmann, R., Roggenbuck, M., Schelhorn, D., Weckmüller, J., Küsel, K., Totsche, K. U., Trumbore, S., and Hildebrandt, A.: Vegetation impacts soil water content patterns by shaping canopy water fluxes and soil properties, Hydrological Processes, 31, 3783–3795, https://doi.org/10.1002/hyp.11274, 2017.
Metzger, J. C., Schumacher, J., Lange, M., and Hildebrandt, A.: Neighbourhood and stand structure affect stemflow generation in a heterogeneous deciduous temperate forest, Hydrology and Earth System Sciences, 23, https://doi.org/10.5194/hess-23-4433-2019, 2019.
Metzger, J. C., Filipzik, J., Michalzik, B., and Hildebrandt, A.: Stemflow Infiltration Hotspots Create Soil Microsites Near Tree Stems in an Unmanaged Mixed Beech Forest, Frontiers in Forests and Global Change, 4, 1–14, https://doi.org/10.3389/ffgc.2021.701293, 2021.
Molina, A. J., Llorens, P., Garcia-Estringana, P., Moreno de las Heras, M., Cayuela, C., Gallart, F., and Latron, J.: Contributions of throughfall, forest and soil characteristics to near-surface soil water-content variability at the plot scale in a mountainous Mediterranean area, Science of The Total Environment, 647, 1421–1432, https://doi.org/10.1016/j.scitotenv.2018.08.020, 2019.
Murray, S. J.: Trends in 20th century global rainfall interception as simulated by a dynamic global vegetation model: Implications for global water resources, Ecohydrology, 7, 102–114, https://doi.org/10.1002/eco.1325, 2014.
Nakagawa, S. and Schielzeth, H.: A general and simple method for obtaining R^2 from generalized linear mixed-effects models, Methods Ecol Evol, 4, 133–142, https://doi.org/10.1111/j.2041-210x.2012.00261.x, 2013.
Nespoulous, J., Merino-Martín, L., Monnier, Y., Bouchet, D. C., Ramel, M., Dombey, R., Viennois, G., Mao, Z., Zhang, J.-L., Cao, K.-F., Le Bissonnais, Y., Sidle, R. C., and Stokes, A.: Tropical forest structure and understorey determine subsurface flow through biopores formed by plant roots, CATENA, 181, 104061, https://doi.org/10.1016/j.catena.2019.05.007, 2019.
Nimmo, J. R.: The processes of preferential flow in the unsaturated zone, Soil Science Society of America Journal, 85, 1–27, https://doi.org/10.1002/saj2.20143, 2021.
Oda, T., Egusa, T., Ohte, N., Hotta, N., Tanaka, N., Green, M. B., and Suzuki, M.: Effects of changes in canopy interception on stream runoff response and recovery following clear-cutting of a Japanese coniferous forest in Fukuroyamasawa Experimental Watershed in Japan, Hydrological Processes, 35, 1–14, https://doi.org/10.1002/hyp.14177, 2021.
Papritz, A. and Schwierz, C.: Package 'georob,' 2020.
Park, A. and Cameron, J. L.: The influence of canopy traits on throughfall and stemflow in five tropical trees growing in a Panamanian plantation, Forest Ecology and Management, 255, 1915–1925, https://doi.org/10.1016/j.foreco.2007.12.025, 2008.
Pebesma, E. J.: Multivariable geostatistics in S: the gstat package, Computers & Geosciences, 30, 683–691, https://doi.org/10.1016/j.cageo.2004.03.012, 2004.

https://doi.org/10.5194/hess-2022-418
Preprint. Discussion started: 6 January 2023

Hydrology and Earth System Sciences
Discussions
Open Access
EGU

795 Pressland, A. J.: Soil Moisture Redistribution as Affected by Throughfall and Stemflow in an Arid Zone Shrub
796 Community, Australian Journal of Botany, 24, 641–649, 1976.
797 Raat, K. J., Draaijers, G. P. J., Schaap, M. G., Tietema, A., and Verstraten, J. M.: Spatial variability of
798 throughfall water and chemistry and forest floor water content in a Douglas fir forest stand, Hydrology
799 and Earth System Sciences, 6, 363–374, https://doi.org/10.5194/hess-6-363-2002, 2002.
800 Ribeiro Jr, P. J. and Diggle, P. J.: geoR: A Package for Geostatistical Analysis, R-NEWS, 1, 15–18, 2001.
801 Rodrigues, A. F., Terra, M. C. N. S., Mantovani, V. A., Cordeiro, N. G., Ribeiro, J. P. C., Guo, L., Nehren, U.,
802 Mello, J. M., and Mello, C. R.: Throughfall spatial variability in a neotropical forest: Have we correctly
803 accounted for time stability?, Journal of Hydrology, 608, https://doi.org/10.1016/j.jhydrol.2022.127632,
804 2022.
805 Rosenbaum, U., Bogena, H. R., Herbst, M., Huisman, J. A., Peterson, T. J., Weuthen, A., Western, A. W., and
806 Vereecken, H.: Seasonal and event dynamics of spatial soil moisture patterns at the small catchment
807 scale, Water Resources Research, 48, W10544, https://doi.org/10.1029/2011WR011518, 2012.
808 Savenije, H. H. G.: The importance of interception and why we should delete the term evapotranspiration from
809 our vocabulary, Hydrological Processes, 18, 1507–1511, https://doi.org/10.1002/hyp.5563, 2004.
810 Schrumpf, M., Kaiser, K., and Schulze, E.-D.: Soil Organic Carbon and Total Nitrogen Gains in an Old Growth
811 Deciduous Forest in Germany, PLoS ONE, 9, e89364, https://doi.org/10.1371/journal.pone.0089364,
812 2014.
813 Schume, H., Jost, G., and Katzensteiner, K.: Spatio-temporal analysis of the soil water content in a mixed
814 Norway spruce (Picea abies (L.) Karst.)-European beech (Fagus sylvatica L.) stand, Geoderma, 112, 273–
815 287, https://doi.org/10.1016/S0016-7061(02)00311-7, 2003.
816 Schwärzel, K., Menzer, A., Clausnitzer, F., Spank, U., Häntzschel, J., Grünwald, T., Köstner, B., Bernhofer, C.,
817 and Feger, K. H.: Soil water content measurements deliver reliable estimates of water fluxes: A
818 comparative study in a beech and a spruce stand in the Tharandt forest (Saxony, Germany), Agricultural
819 and Forest Meteorology, 149, 1994–2006, https://doi.org/10.1016/j.agrformet.2009.07.006, 2009.
820 Shachnovich, Y., Berliner, P. R., and Bar, P.: Rainfall interception and spatial distribution of throughfall in a
821 pine forest planted in an arid zone, Journal of Hydrology, 349, 168–177,
822 https://doi.org/10.1016/j.jhydrol.2007.10.051, 2008.
823 Staelens, J., De Schrijver, A., Verheyen, K., and Verhoest, N. E. C.: Spatial variability and temporal stability of
824 throughfall water under a dominant beech (Fagus sylvatica L.) tree in relationship to canopy cover,
825 Journal of Hydrology, 330, 651–662, https://doi.org/10.1016/j.jhydrol.2006.04.032, 2006.
826 Staelens, J., De Schrijver, A., Verheyen, K., and Verhoest, N. E. C.: Rainfall partitioning into throughfall,
827 stemflow, and interception within a single beech (Fagus sylvatica L.) canopy: influence of foliation, rain
828 event characteristics, and meteorology, Hydrological Processes, 22, 33–45, https://doi.org/10.1002/hyp,
829 2008.
830 Su, L., Xie, Z., Xu, W., and Zhao, C.: Variability of throughfall quantity in a mixed evergreen-deciduous
831 broadleaved forest in central China, Journal of Hydrology and Hydromechanics, 67, 225–231,
832 https://doi.org/10.2478/johh-2019-0008, 2019.
833 Vachaud, G., Passerat De Silans, A., Balabanis, P., and Vauclin, M.: Temporal Stability of Spatially Measured
834 Soil Water Probability Density Function, Soil Science Society of America Journal, 49, 822–828,
835 https://doi.org/10.2136/sssaj1985.03615995004900040006x, 1985.
836 Van Stan, J. T., Lewis, E. S., Hildebrandt, A., Rebmann, C., and Friesen, J.: Impact of interacting bark structure
837 and rainfall conditions on stemflow variability in a temperate beech-oak forest, central Germany,
838 Hydrological Sciences Journal, 61, 2071–2083, https://doi.org/10.1080/02626667.2015.1083104, 2016.
839 Van Stan, J. T., Hildebrandt, A., Friesen, J., Metzger, J. C., and Yankine, S. A.: Spatial Variability and Temporal
840 Stability of Local Net Precipitation Patterns, in: Precipitation Partitioning by Vegetation, edited by: Van
841 Stan, II, J. T., Gutmann, E., and Friesen, J., Springer International Publishing, Cham, 89–104,
842 https://doi.org/10.1007/978-3-030-29702-2_6, 2020.
843 Vereecken, H., Kamai, T., Harter, T., Kasteel, R., Hopmans, J., and Vanderborght, J.: Explaining soil moisture
844 variability as a function of mean soil moisture: A stochastic unsaturated flow perspective, Geophysical
845 Research Letters, 34, 1–6, https://doi.org/10.1029/2007GL031813, 2007.
846 Voss, S., Zimmermann, B., and Zimmermann, A.: Detecting spatial structures in throughfall data: The effect of
847 extent, sample size, sampling design, and variogram estimation method, Journal of Hydrology, 540, 527–
848 537, https://doi.org/10.1016/j.jhydrol.2016.06.042, 2016.
849 Western, A. W., Zhou, S. L., Grayson, R. B., McMahon, T. A., Blöschl, G., and Wilson, D. J.: Spatial correlation
850 of soil moisture in small catchments and its relationship to dominant spatial hydrological processes,
851 Journal of Hydrology, 286, 113–134, https://doi.org/10.1016/j.jhydrol.2003.09.014, 2004.
852 Wullaert, H., Pohlert, T., Boy, J., Valarezo, C., and Wilcke, W.: Spatial throughfall heterogeneity in a montane
853 rain forest in Ecuador: Extent, temporal stability and drivers, Journal of Hydrology, 377, 71–79,
854 https://doi.org/10.1016/j.jhydrol.2009.08.001, 2009.
855 Zehe, E., Graeff, T., Morgner, M., Bauer, a., and Bronstert, a.: Plot and field scale soil moisture dynamics and
856 subsurface wetness control on runoff generation in a headwater in the Ore Mountains, Hydrology and

https://doi.org/10.5194/hess-2022-418
Preprint. Discussion started: 6 January 2023

857 Earth System Sciences, 14, 873–889, https://doi.org/10.5194/hess-14-873-2010, 2010.
858 Zhu, X., He, Z., Du, J., Chen, L., Lin, P., and Tian, Q.: Spatial heterogeneity of throughfall and its contributions
859 to the variability in near-surface soil water-content in semiarid mountains of China, Forest Ecology and
860 Management, 488, https://doi.org/10.1016/j.foreco.2021.119008, 2021.
861 Zimmermann, A. and Zimmermann, B.: Requirements for throughfall monitoring: The roles of temporal scale
862 and canopy complexity, Agricultural and Forest Meteorology, 189–190, 125–139,
863 https://doi.org/10.1016/j.agrformet.2014.01.014, 2014.
864 Zimmermann, A., Germer, S., Neill, C., Krusche, A. V., and Elsenbeer, H.: Spatio-temporal patterns of
865 throughfall and solute deposition in an open tropical rain forest, Journal of Hydrology, 360, 87–102,
866 https://doi.org/10.1016/j.jhydrol.2008.07.028, 2008.
867 Zimmermann, A., Zimmermann, B., and Elsenbeer, H.: Rainfall redistribution in a tropical forest: Spatial and
868 temporal patterns, Water Resources Research, 45, 1–18, https://doi.org/10.1029/2008WR007470, 2009.
869 Zimmermann, A., Voss, S., Metzger, J. C., Hildebrandt, A., and Zimmermann, B.: Capturing heterogeneity: The
870 role of a study area's extent for estimating mean throughfall, Journal of Hydrology, 542, 781–789,
871 https://doi.org/10.1016/j.jhydrol.2016.09.047, 2016.
872 Zimmermann, B., Zimmermann, A., Lark, R. M., and Elsenbeer, H.: Sampling procedures for throughfall
873 monitoring: A simulation study, Water Resources Research, 46, 1–15,
874 https://doi.org/10.1029/2009WR007776, 2010.

875